

cases, reflect a change in the nuclear structure at large angular momenta (above the 8^+ state in the present case) that is abrupt enough to slow down the electromagnetic decay.

It is also interesting to study the observed side-feeding times. In all decay curves we observed long components (cf. Fig. 1) which, however, down to the 8^+ state seem to be mainly artifacts of the long tail of the initial $14^+ \rightarrow 12^+$ decay. Another long side-feeding component is, however, definitely observed for the $8^+ \rightarrow 6^+$ transition and this component contains nearly 75% of the total side-feeding intensity to the 8^+ state. In this case the particular side-feeding transition could be identified as the 397-keV γ ray observed in Ref. 6. The properties of the 3208-keV state from which it originates are not known. However, from the γ - γ coincidence spectra and the measured γ -ray intensities of Ref. 6 it can be concluded that neither is this level populated by transitions from the higher-lying yrast states nor does it decay with a noticeable fraction to any yrast state other than the 8^+ state. It therefore appears that the 3208-keV state is the endpoint of γ cascades between states of which the configurations are quite different from those of the yrast states. This supports the conclusion that ^{134}Ce experiences a drastic change in structure above the 8^+ state of the yrast sequence. To our knowledge ^{134}Ce is the first nucleus where a strong backbending and a strong retardation of the electromagnetic

decay rates of the yrast states has been observed.

One of us (J. S. Mills) thanks the Max-Planck-Gesellschaft for making his stay in Heidelberg possible.

†Work supported in part by Bundesministerium für Forschung und Technologie.

*On leave from National Physical Research Laboratory, Council for Scientific Industrial Research, Pretoria, South Africa.

¹D. Ward, in *Proceedings of the International Conference on Reactions between Complex Nuclei, Nashville, Tennessee, 1974*, edited by R. L. Robinson, F. K. McGowan, J. B. Ball, and J. H. Hamilton (North-Holland, Amsterdam, 1974), Vol. 2 p. 417.

²D. Ward, H. R. Andrews, J. S. Geiger, R. L. Graham, and J. F. Sharpey-Schafer, *Phys. Rev. Lett.* **30**, 493 (1973).

³B. Bochev, R. Kalpakchieva, S. A. Karamian, T. Kutsarova, E. Nadjakov, and V. G. Subbotin, Joint Institute for Nuclear Research, Dubna Reports No. P7-8531 and No. P7-8567 (to be published).

⁴F. Kearns, G. D. Dracoulis, T. Inamura, J. C. Lisle, and J. C. Willmott, *J. Phys. A* **7**, L11 (1974).

⁵D. Husar, J. S. Mills, H. Gräf, U. Neumann, and D. Pelte, to be published.

⁶W. Dehnhardt, J. S. Mills, M. Müller-Veggian, U. Neumann, D. Pelte, G. Poggi, B. Povh, and P. Taras, *Nucl. Phys.* **A225**, 1 (1974).

⁷D. B. Fossan and E. K. Warburton, in *Nuclear Spectroscopy and Reactions*, edited by Joseph Cerny (Academic, New York, 1974), Pt. C, p. 307.

Comparisons of Proton and Neutron Transfer Reactions and Explicit Coulomb Effects*

K. G. Nair, K. Nagatani, and H. Voit†

Cyclotron Institute, Texas A&M University, College Station, Texas 77843

(Received 24 March 1976)

Experimental and theoretical ratios of pairs of heavy-ion direct reactions of the form $A(a, b)B$ and $A(a, B)b$ where b and B are isobaric nuclei could be used to highlight the Coulomb effects on the neutron and proton form factors in a unique manner. These results quantitatively provide evidence for the need for including the Coulomb potentials in the interaction that causes transfer previously studied in terms of the theoretical post-prior equality of the transition amplitude.

A comparative study of direct analog-channel reactions of the form $A(a, b)B$ and $A(a, b')B'$ where the nuclei (b, b') and (B, B') are pairs of analog nuclei has been made to investigate the explicit role of the Coulomb effects involved. In fact, such studies have been made recently using the (d, t) and $(d, {}^3\text{He})$ reactions¹ on a number of self-conjugate nuclei. It was found in these reac-

tions that the proton- and neutron-transfer differential cross sections were different in general and that this could be explained most probably as due to the differences in Q values and in the bound-state wave functions of the transferred neutron and proton. A similar study² was also made using the reactions ${}^{14}\text{N}({}^6\text{Li}, {}^7\text{Li}){}^{13}\text{N}$ and ${}^{14}\text{N}({}^6\text{Li}, {}^7\text{Be}){}^{13}\text{C}$.

In the present investigation we impose an additional important restriction on the types of reactions studied so that many ambiguities inherent in the theoretical treatments may be eliminated. This consists of demanding that $b = B'$ and $b' = B$ in the exit channel. Moreover, we restrict our attention to single-nucleon transfers only. For such reactions, the final scattering wave functions for these two processes are of course common. Thus the appropriate cross sections can be written somewhat symbolically using the usual distorted-wave Born approximation (DWBA) as

$$\sigma_N \sim |\langle \chi_f | F_N | \chi_i \rangle|^2,$$

where χ_i and χ_f are the distorted waves in the incident and exit channels, respectively, and F_N is the corresponding nucleon-transfer form factor. Now the difference between the proton- and neutron-transfer reactions is only in the form factor F_N . However, a word of caution is in order here. The angular distributions of these reactions must be extremely forward-peaked (which is the case for heavy-ion reactions far above the Coulomb barrier in general, and true for the particular cases studied here, as will be seen later) so that the interference between the amplitudes corresponding to the outgoing nuclei detected at angle θ and the recoil of its analog reaction detected at angle $\pi - \theta$ could be neglected. It may be worth mentioning here that this special class of nuclear reactions have been studied from a macroscopic point of view by Barshay and Temmer.³ In the present situation, we focus our attention on the microscopic picture in which the isobaric

multiplet states and the interactions which cause the transfers demonstrate explicit differences due to the Coulomb effects.

We present here the results⁴ taken with 155-MeV ^{14}N beams and 100-MeV ^{10}B beams on ^{12}C , ^{16}O , and ^{14}N targets at the Texas A&M University Cyclotron Institute. An example of the experimental angular distributions obtained and the corresponding exact finite range (EFR) DWBA fits⁵ for $^{12}\text{C}(^{10}\text{B}, ^{11}\text{B})^{11}\text{C}(\text{g.s.})$ and $^{12}\text{C}(^{10}\text{B}, ^{11}\text{C})^{11}\text{B}(\text{g.s.})$ at 100 MeV are shown in Fig. 1. Note the near exponential falloff of the angular distributions from extreme forward angles, a condition necessary for the validity of the arguments given above. Also shown are the experimental and theoretical ratios of the proton- to neutron-transfer differential cross sections (denoted as R in the figure) for three of the reactions studied where the vertical bars on the data points indicate the statistical errors in the measurements. It should be emphasized that from an experimental standpoint, such ratio measurements of different outgoing channels from a single incident channel in a given experiment eliminate a number of possible spurious errors. It is seen that the experimental ratios are close to unity whereas the calculated ratios indicated by dotted curves in the figure are conspicuously displaced. This suggests that some fundamental defects are built into the theoretical calculations. An immediate but rather arbitrary solution to this problem is to change the nuclear part of the bound-state geometry of the proton relative to that of the neutron in the two systems and a fit to the experimental

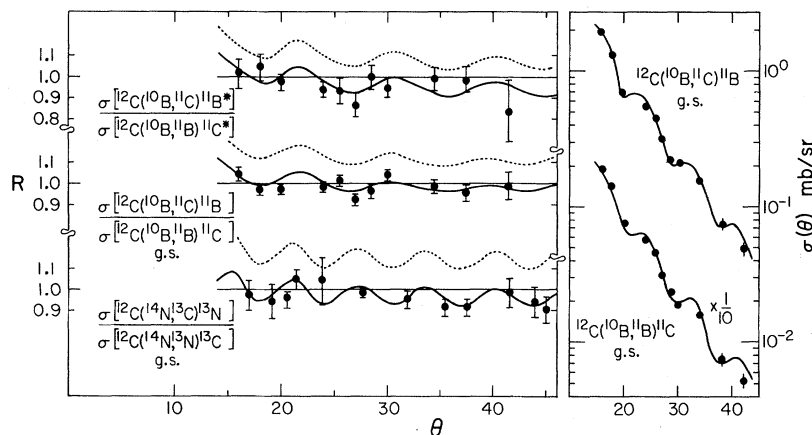


FIG. 1. Averaged ratio R versus θ (left-hand side) for the first three sets of reactions shown in Table I. The dotted lines indicate EFR DWBA calculations without the Coulomb terms in the perturbing potential. The continuous curves indicate calculations after including these terms. The right-hand side illustrates the quality of the EFR DWBA fits to the experimental data for the specific reactions shown. The error bars on the data points are statistical in origin.

results could indeed be obtained. However, there is no basic theoretical or experimental evidence to support such a procedure (note that we are considering analog states).

A more plausible explanation for these discrepancies is perhaps based on the imperfect treatment of the Coulomb part of the interaction^{6,7} that causes the transfers. In fact, DeVries, Satchler, and Cramer⁷ have stressed the importance of such terms in the DWBA form factor to satisfactorily account for the expected post-prior equality of the transition amplitude. These terms can be written, for example, for a stripping reaction $A(a, b)B$ (with $a = b + x$ and $B = A + x$) in the post-representation as

$$\Delta V^c = V_{bx}^c(r_{bx}) + V_{ba}^c(r_{ba}) - V_{bB}^c(r_b),$$

where the radial forms are assumed to have the well-known dependence of the Coulomb potential for a uniform spherical charge distribution. The nuclear part of the interaction is⁷ then

$$\Delta V^n = V_{bx}^n(r_{bx}) + V_{ba}^n(r_{ba}) - U_{bB}^n(r_b),$$

where V and U denote the appropriate nuclear and optical potentials, respectively. The total interaction potential is $\Delta V = \Delta V^n + \Delta V^c$.

Calculations were repeated after the inclusion of the Coulomb terms and the corresponding results are indicated by continuous lines in Fig. 1. The excellent agreement with the data is now obvious. This emphasizes the importance of the Coulomb interaction terms in heavy-ion transfer reactions. It should be mentioned in passing that the difference $V_{ba}^n - U_{bB}^n$ has been ignored in the present calculations since the exact form of V_{ba}^n is unknown. (This part of the interaction has

been shown to be insignificant for single-nucleon transfers.⁷) Calculations were also performed using the post and prior forms of the transition amplitude with agreement to within 1% for the reactions shown.

The same procedures were then applied to the reactions where the final nuclei are not isobaric multiplets, such as $^{12}\text{C}(^{10}\text{B}, ^{11}\text{C})^{11}\text{B}^*(2.14)$ versus $^{12}\text{C}(^{10}\text{B}, ^{11}\text{B})^{11}\text{C}^*(1.99)$ (Fig. 1), $^{16}\text{O}(^{14}\text{N}, ^{13}\text{C})^{17}\text{F}$ -(g.s.) versus $^{16}\text{O}(^{14}\text{N}, ^{13}\text{N})^{17}\text{O}$ (g.s.), and $^{14}\text{N}(^{10}\text{B}, ^{11}\text{C})^{13}\text{C}$ (g.s.) versus $^{14}\text{N}(^{10}\text{B}, ^{11}\text{B})^{13}\text{N}$ (g.s.). In these cases the Q -value differences and differences in the nonidentical exit channels produce some complications. However, similar features were observed in these reactions as well, and the inclusion of the Coulomb terms significantly improved the agreement between theory and experiment. These results are summarized in Table I.

As mentioned before, the experimental proton- and neutron-transfer cross sections were rather close to each other. This is in contrast to the findings from light-ion reactions.¹ It is in essence a reflection of the localization of heavy-ion transfer near the surface regions of the colliding nuclei where the proton and neutron form factors are close. This should be compared to the situation in light-ion reactions where, in the absence of such a localization, the different radial dependences of the proton and neutron form factors are manifested through the correspondingly different differential cross sections.

To summarize, a comparative study of several proton- and neutron-transfer reactions has been made. The ratios of the experimental cross sections were in general found to be close to unity which is a consequence of the tight localization

TABLE I. Ratios of proton to neutron transfer differential cross sections.

Systems	E (MeV)	R^a (EFR DWBA)		R^a (Expt.)
		No Coulomb	With Coulomb	
$^{12}\text{C}(^{14}\text{N}, ^{13}\text{C})^{13}\text{N}$ (g.s.)	155	1.18	0.98	0.97 ± 0.06
$^{12}\text{C}(^{14}\text{N}, ^{13}\text{N})^{13}\text{C}$ (g.s.)				
$^{12}\text{C}(^{10}\text{B}, ^{11}\text{C})^{11}\text{B}$ (g.s.)	100	1.13	0.98	0.98 ± 0.03
$^{12}\text{C}(^{10}\text{B}, ^{11}\text{B})^{11}\text{C}$ (g.s.)				
$^{12}\text{C}(^{10}\text{B}, ^{11}\text{C})^{11}\text{B}$ (2.14)	100	1.15	0.99	0.95 ± 0.08
$^{12}\text{C}(^{10}\text{B}, ^{11}\text{B})^{11}\text{C}$ (1.99)				
$^{16}\text{O}(^{14}\text{N}, ^{13}\text{C})^{17}\text{F}$ (g.s.)	155	1.22	0.96	0.83 ± 0.07
$^{16}\text{O}(^{14}\text{N}, ^{13}\text{N})^{17}\text{O}$ (g.s.)				
$^{14}\text{N}(^{10}\text{B}, ^{11}\text{C})^{13}\text{C}$ (g.s.)	97	1.23	1.08	0.92 ± 0.09
$^{14}\text{N}(^{10}\text{B}, ^{11}\text{B})^{13}\text{N}$ (g.s.)				

^a Averaged values over the range of measured angles.

of the reaction amplitude near the nuclear surface for heavy-ion reactions. Application of the EFR DWBA showed excellent agreement with experimental results provided the Coulomb interaction in the perturbing potential is properly taken into account. Of course, in principle, the very small charge-dependent nuclear interactions will also play a role in these comparisons. But the current levels of sophistication of both theory and experiment are not sufficient to warrant these considerations in our present results. Since the choice was made such that a number of ambiguities present in usual direct-reaction studies were minimized, this may be one of the most accurate checks of the DWBA analyses applied to heavy-ion reactions. Extension of such studies to heavier nuclei and also to multinucleon transfers should be fruitful since there the Coulomb effects are expected to be even more important.

We would like to express our appreciation to K. I. Kubo for some useful discussions. A. Bach-

er, C. Towsley, M. Hamm, and R. Hanus are thanked for their help at various stages of this investigation.

*Work supported in part by the National Science Foundation.

†Permanent address: Physikalisches Institut der Universität Erlangen-Nürnberg, Erlangen, W. Germany.

¹R. E. Tribble, to be published.

²K. O. Groeneveld *et al.*, Phys. Rev. Lett. **27**, 1806 (1971).

³S. Barshay and G. M. Temmer, Phys. Rev. Lett. **12**, 728 (1964); also see D. Robson and A. Richter, Ann. Phys. (N.Y.) **63**, 261 (1971).

⁴H. Voit *et al.*, Phys. Lett **58B**, 152 (1975).

⁵K. G. Nair *et al.*, Phys. Rev. C **12**, 1575 (1975).

⁶K. G. Nair *et al.*, Phys. Rev. C **8**, 1129 (1973), and references therein; W. Toboeman *et al.*, Nucl. Phys. **A205**, 193 (1973).

⁷R. M. DeVries, G. R. Satchler, and J. G. Cramer, Phys. Rev. Lett. **32**, 1377 (1974).

Multiphoton Ionization Spectroscopy of High-Lying, Even-Parity States in Calcium*

P. Esherick, J. A. Armstrong, R. W. Dreyfus, and J. J. Wynne
IBM Thomas J. Watson Research Center, Yorktown Heights, New York 10598

(Received 4 December 1975)

Strong ionization signals have been observed in Ca following two-photon absorption to the bound, even-parity $J=0$ and $J=2$ states. Using known Ca absorption lines for calibration, 72 new states have been classified, and their energies have been determined to $\pm 0.1 \text{ cm}^{-1}$. The new $J=0$ states have a constant quantum defect, whereas the $J=2$ states do not.

Two-photon laser spectroscopy has had great impact on the study of excited atomic and molecular states.¹⁻⁴ We have observed strong ionization signals following two-photon absorption of light to 72 previously unknown even-parity $J=0$ and $J=2$ states of Ca. A typical multiphoton ionization spectrum, shown in Fig. 1, illustrates the sensitivity and resolving power of this technique. We have found and identified the $4sns \ ^1S_0$ states from $n=13$ to 30. We have also found 54 $J=2$ states which we have identified as 1D_2 . The $4snd \ ^1D_2$ series is strongly perturbed by interactions with the $3d5s$ and the $(3d)^2 \ ^3P_2$ levels; this has prevented workers using conventional emission spectroscopy⁵ from clearly identifying the " $4snd$ " 1D_2 series for $n > 7$.

The known⁶ $4snp \ ^1P_1^\circ$ states converge to the same limit and therefore are as densely spaced as the $4sns \ ^1S_0$ and " $4snd$ " 1D_2 states. By frequen-

cy doubling the laser and using linear absorption to the $4snp \ ^1P_1^\circ$ levels to provide a series of calibration points, the energies of the newly identified states have been determined to $\pm 0.1 \text{ cm}^{-1}$.

The experimental apparatus consisted of a nitrogen-laser-pumped dye laser,⁷ Ca vapor in a heated cylindrical pipe, and an ionization probe. The laser had a linewidth of 0.5 cm^{-1} , a pulse width of $\sim 10 \text{ nsec}$, and a power of 10–50 kW over the range 4025–4325 Å. The beam was focused into the calcium pipe with intensities, I_L , up to 10^8 W/cm^2 . The pipe was heated from 600 to 800 °C, yielding Ca pressures, P_{Ca} , from ~ 0.015 to 1.0 Torr. Diffusion of the Ca vapor to the cold ends of the pipe was prevented by buffer gas (Ne or Kr) at pressures, P_b , from 5 to 50 Torr. The ionization probe was a tungsten wire (2 mm diam) which extended axially into the hot zone of the Ca pipe. This probe was held at a negative potential,